

Pattern Formation and Spatiotemporal Chaos

Insights from Large Scale Numerical Simulations
of Rayleigh-Bénard convection

Collaborators: Mark Paul, Keng-Hwee Chiam, Janet Scheel, Henry Greenside, Anand Jayaraman, Paul Fischer

Support: DOE; Computer time: NSF, NERSC, NCSA, ANL

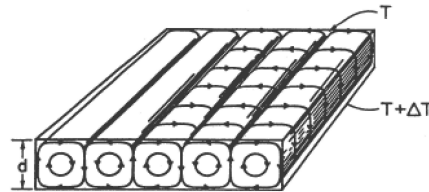
Outline

Use **numerical simulation** of **Rayleigh-Bénard convection** in **realistic** geometries to learn about complex spatial patterns and dynamics in spatially extended systems.

Examples:

- Pattern chaos: power spectrum
- Lyapunov exponents
- Coarsening and wavenumber selection

Rayleigh-Bénard Convection



RBC allows a *quantitative* comparison to be made between theory and experiment.

Nondimensional Boussinesq Equations

- Momentum Conservation

$$\frac{1}{\sigma} \left[\frac{\partial \vec{u}}{\partial t} + (\vec{u} \cdot \vec{\nabla}) \vec{u} \right] = -\vec{\nabla} p + R T \hat{e}_z + \nabla^2 \vec{u} + 2\Omega \hat{e}_z \times \vec{u}$$

- Energy Conservation

$$\frac{\partial T}{\partial t} + (\vec{u} \cdot \vec{\nabla}) T = \nabla^2 T$$

- Mass Conservation

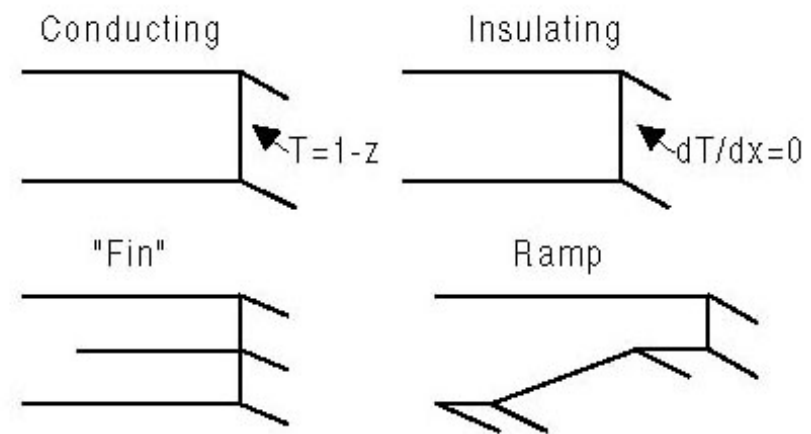
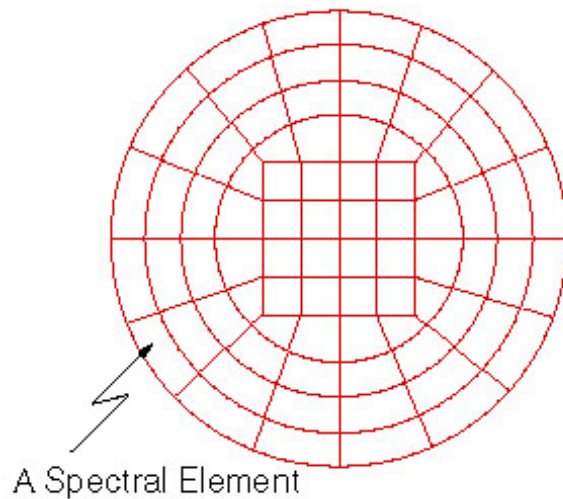
$$\vec{\nabla} \cdot \vec{u} = 0$$

Aspect Ratio: $\Gamma = \frac{r}{h}$

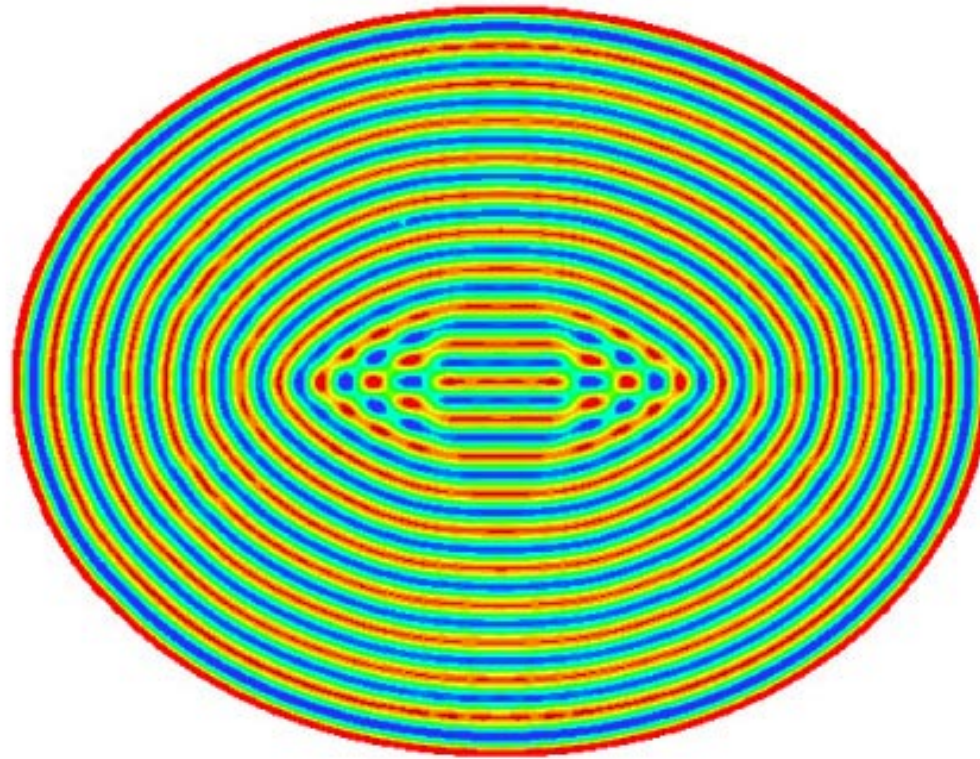
BC: no-slip, insulating or conducting, and constant ΔT

Spectral Element Numerical Solution

- Accurate simulation of long-time dynamics
- Exponential convergence in space, third order in time
- Efficient parallel algorithm, unstructured mesh
- Arbitrary geometries, realistic boundary conditions



Convection in an elliptical container



cf. Ercolani, Indik, and Newell, *Physica D* (2003)

Pattern chaos: convection in small cylindrical geometries

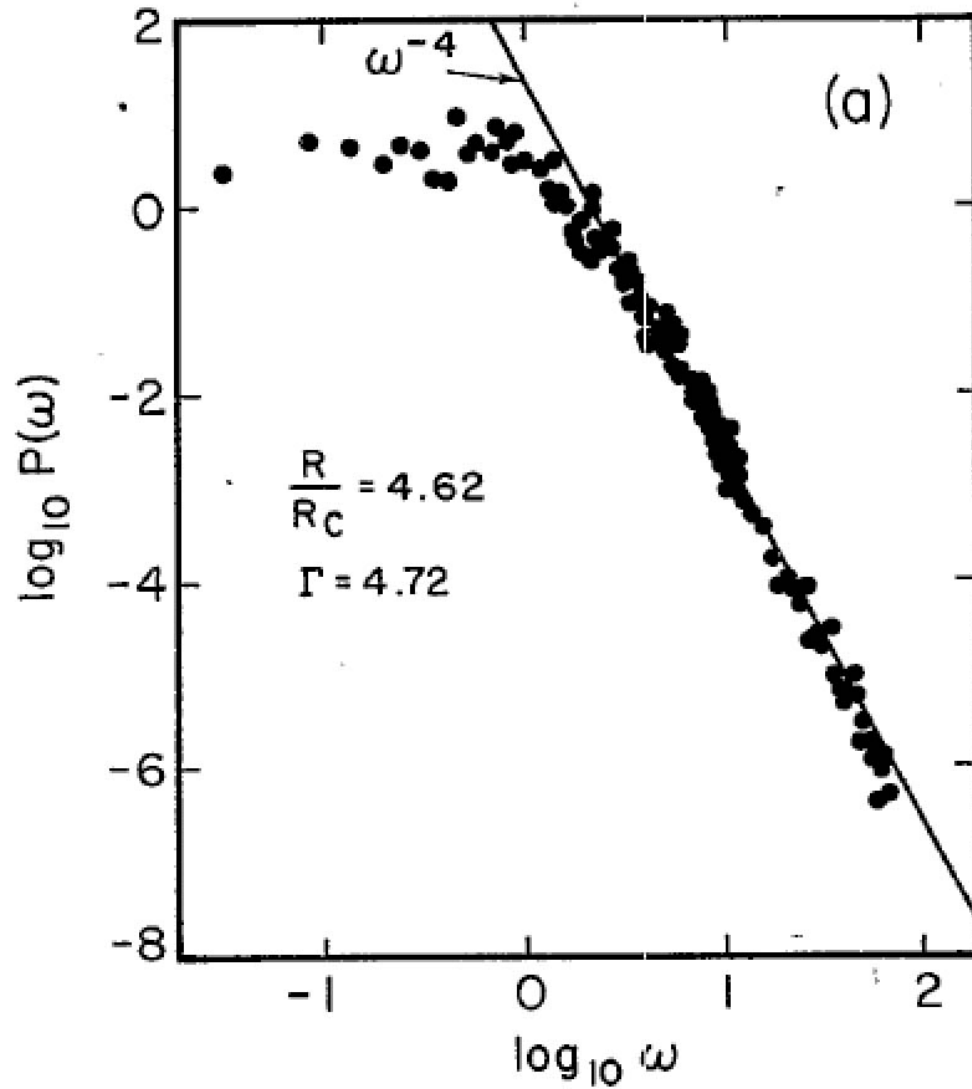
- First experiments: $\Gamma = 5.27$ cell, cryogenic (normal) liquid He^4 as fluid. High precision heat flow measurements (no flow visualization).
- Onset of aperiodic time dependence in low Reynolds number flow: relevance of chaos to “real” (continuum) systems.
- Power law decrease of power spectrum $P(f) \sim f^{-4}$

G. Ahlers, Phys. Rev. Lett. **30**, 1185 (1974)

G. Ahlers and R.P. Behringer, Phys. Rev. Lett. **40**, 712 (1978)

H. Gao and R.P. Behringer, Phys. Rev. A**30**, 2837 (1984)

V. Croquette, P. Le Gal, and A. Pocheau, Phys. Scr. T**13**, 135 (1986)

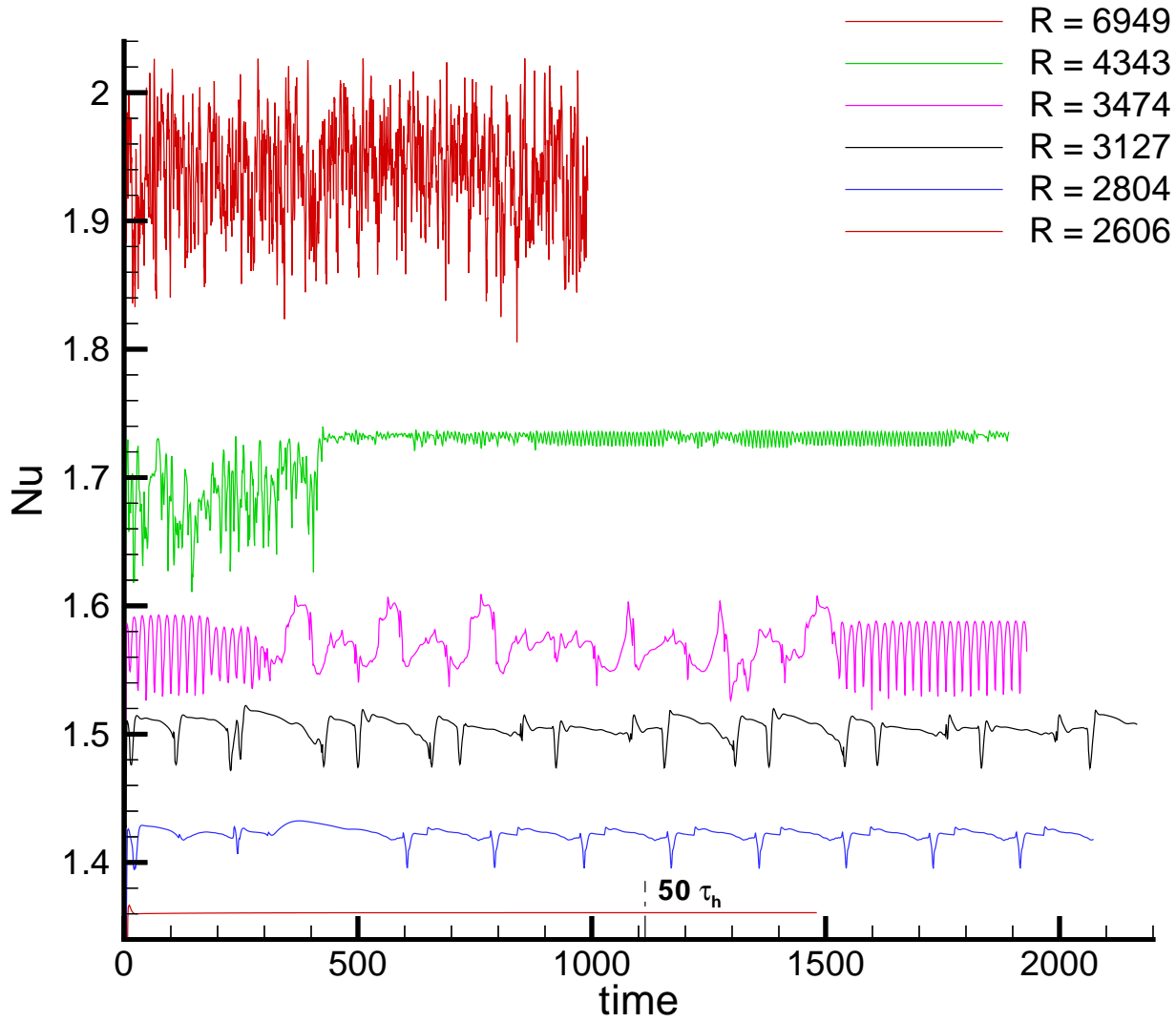


(from Ahlers and Behringer 1978)

Numerical Simulations

- $\Gamma = 4.72, \sigma = 0.78, 2600 \lesssim R \lesssim 7000$
- Conducting sidewalls
- Random thermal perturbation initial conditions
- Simulation time $\sim 100\tau_h$
 - Simulation time ~ 12 hours on 32 processors
 - Experiment time ~ 172 hours or ~ 1 week

$\Gamma = 4.72$
 $\sigma = 0.78$ (Helium)
 Random Initial Conditions



$$R = 3127$$

$$R = 6949$$

Power Spectrum

- Simulations of **low dimensional chaos** (e.g. Lorenz model) show exponential decaying power spectrum
- Power law power spectrum easily obtained from **stochastic** models (white-noise driven oscillator, etc.)

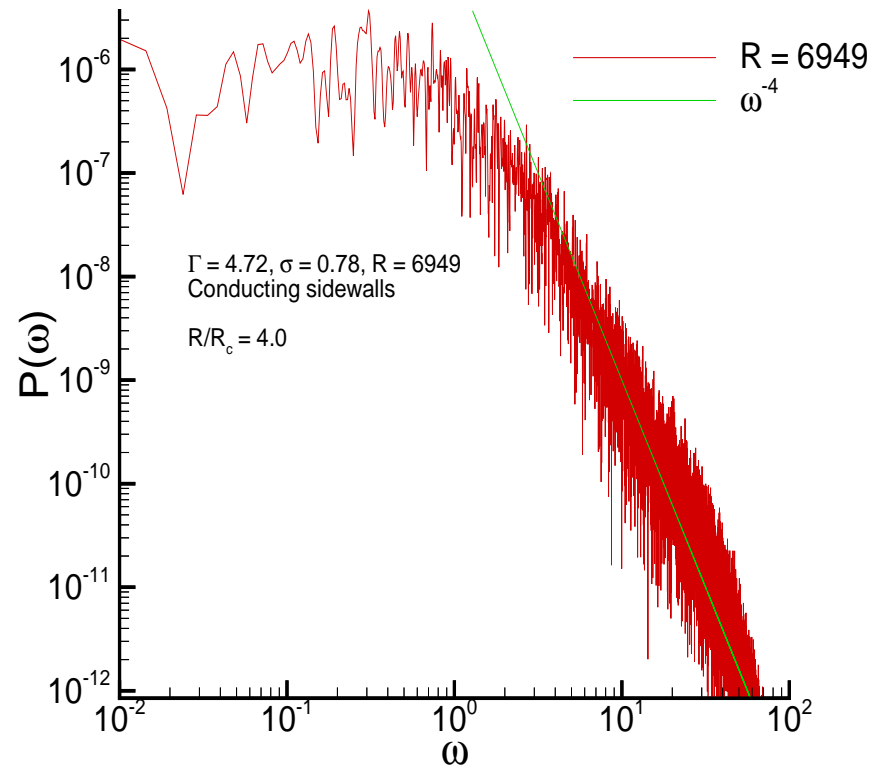
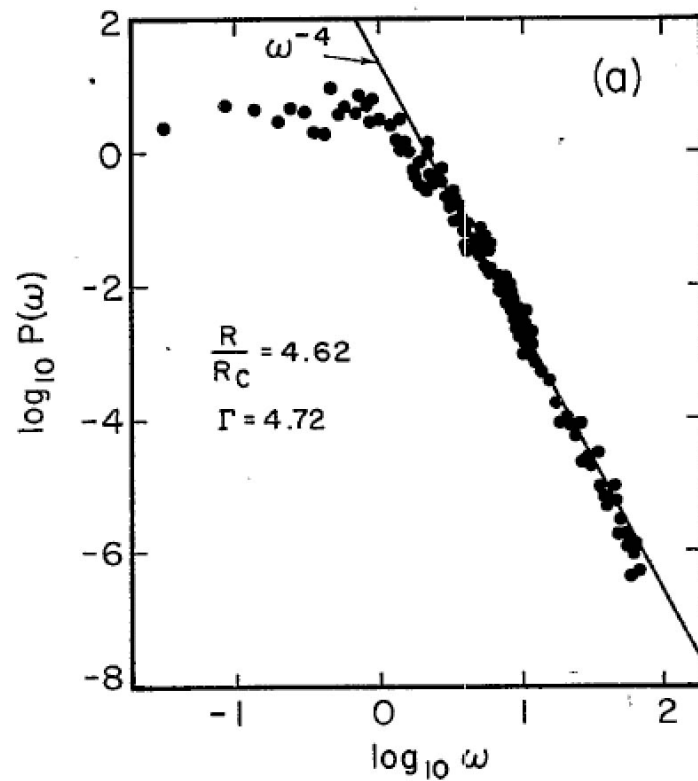
Power Spectrum

- Simulations of **low dimensional chaos** (e.g. Lorenz model) show exponential decaying power spectrum
- Power law power spectrum easily obtained from **stochastic** models (white-noise driven oscillator, etc.)

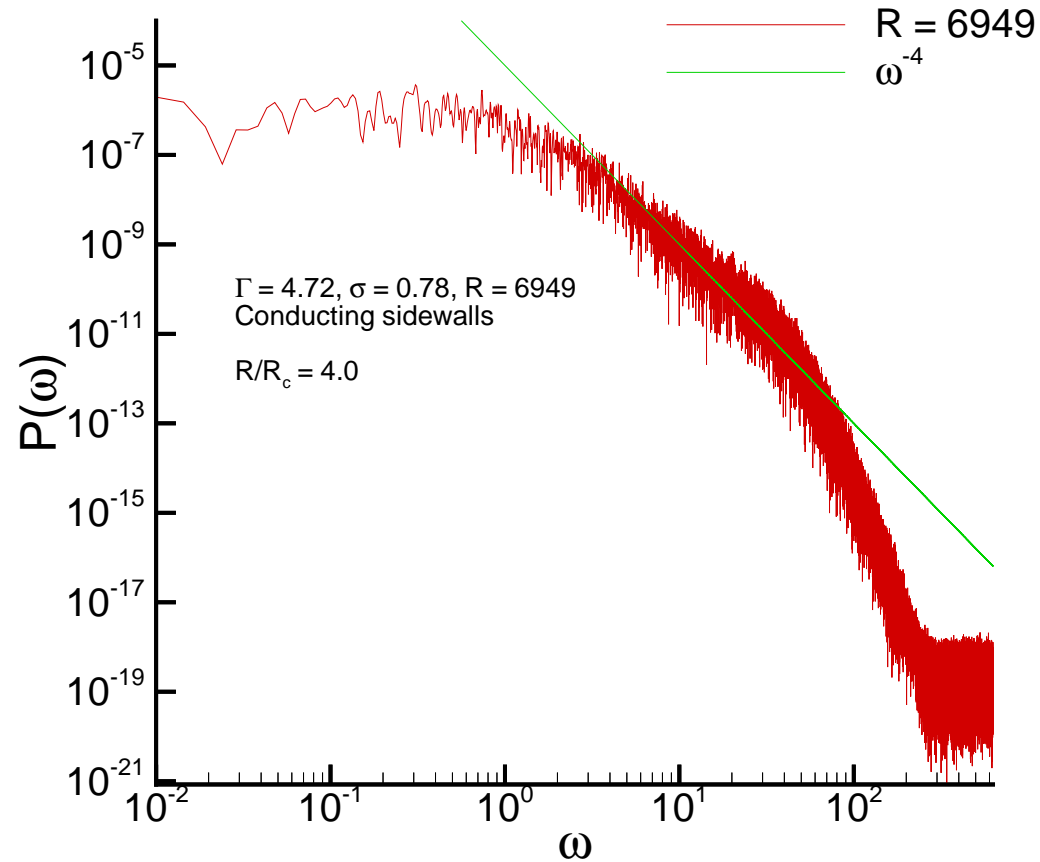
Simulation Results

Simulations reproduce experimental results....

Simulation yields a power law over the range accessible to experiment



When larger frequencies are included an exponential tail is found



Exponential tail not seen in experiment because of instrumental noise floor

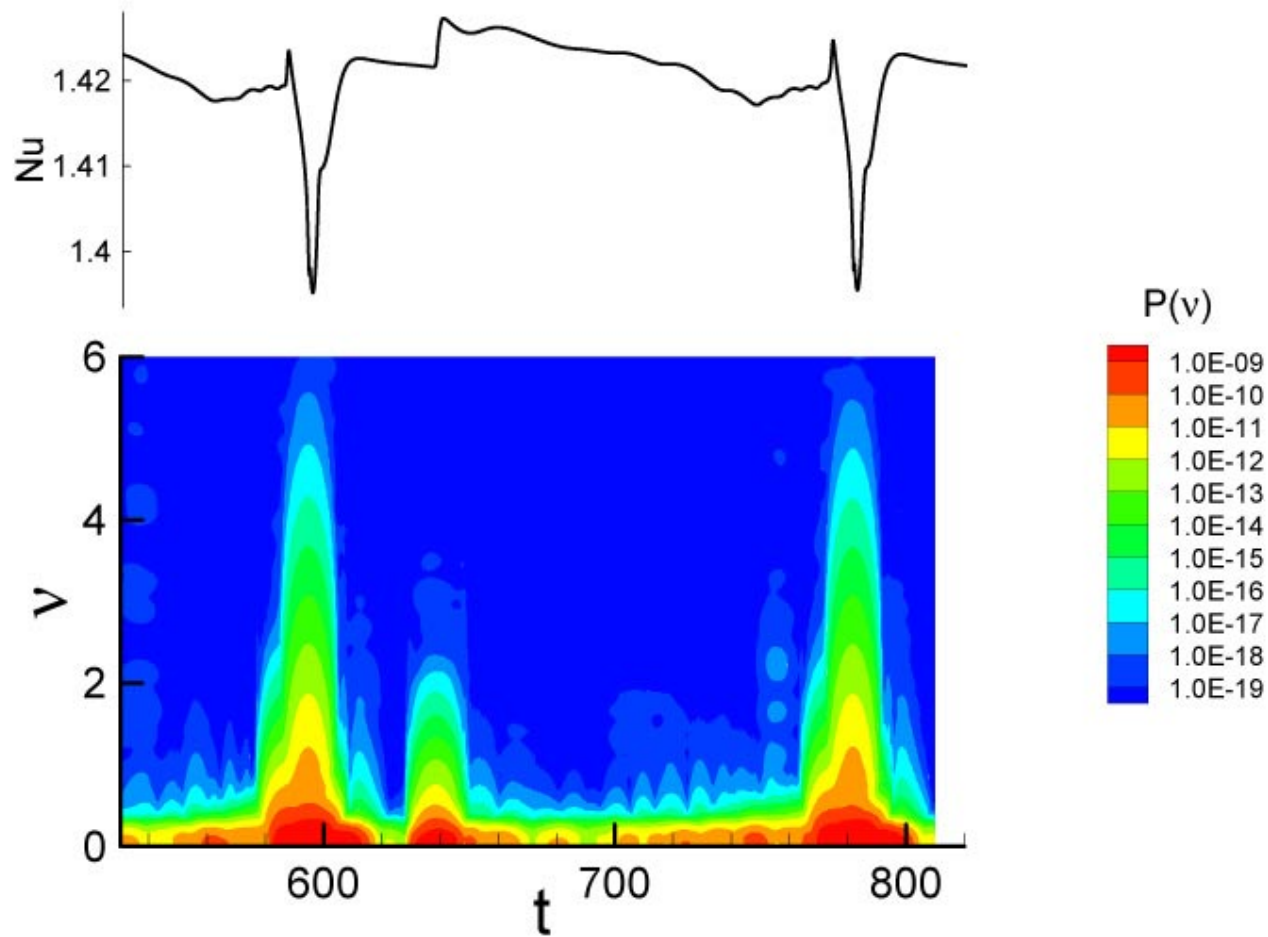
Where does the power law come from?

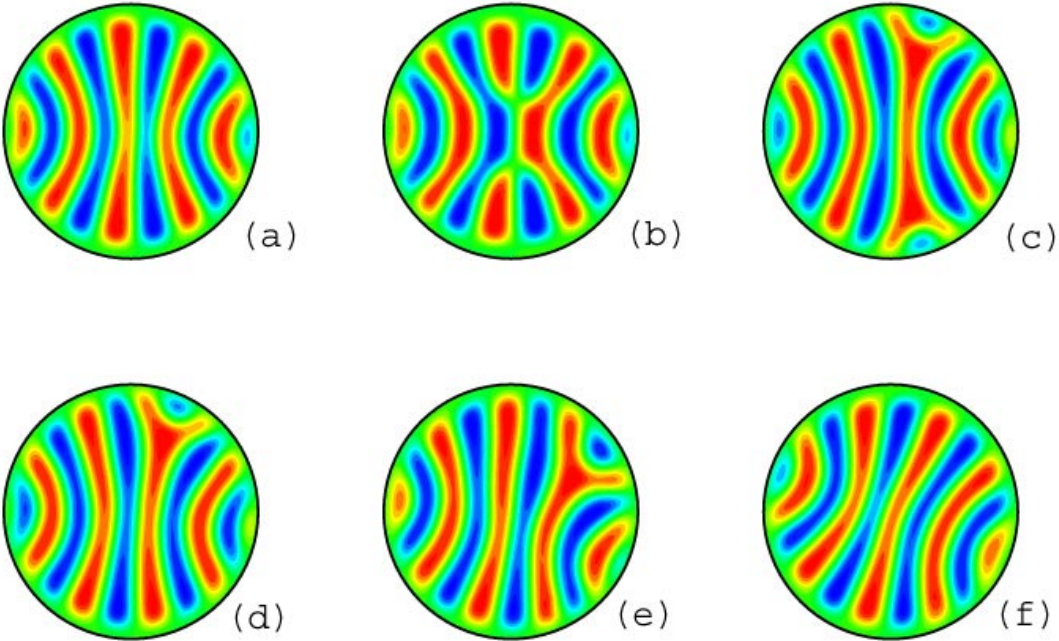
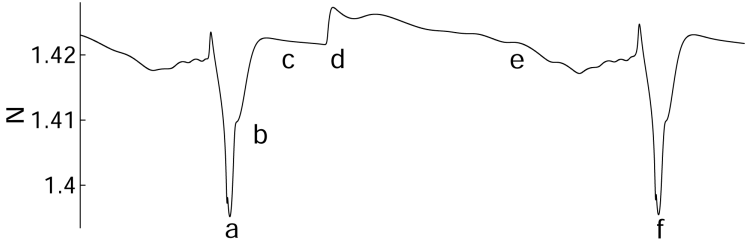
Power law arises from **quasi-discontinuous changes in the slope** of $N(t)$ on a $t = 0.1 - 1$ time scale associated with roll pinch-off events.

This is clearest to see for the low Rayleigh number where the motion is periodic, but again the power spectrum has a power law fall off.

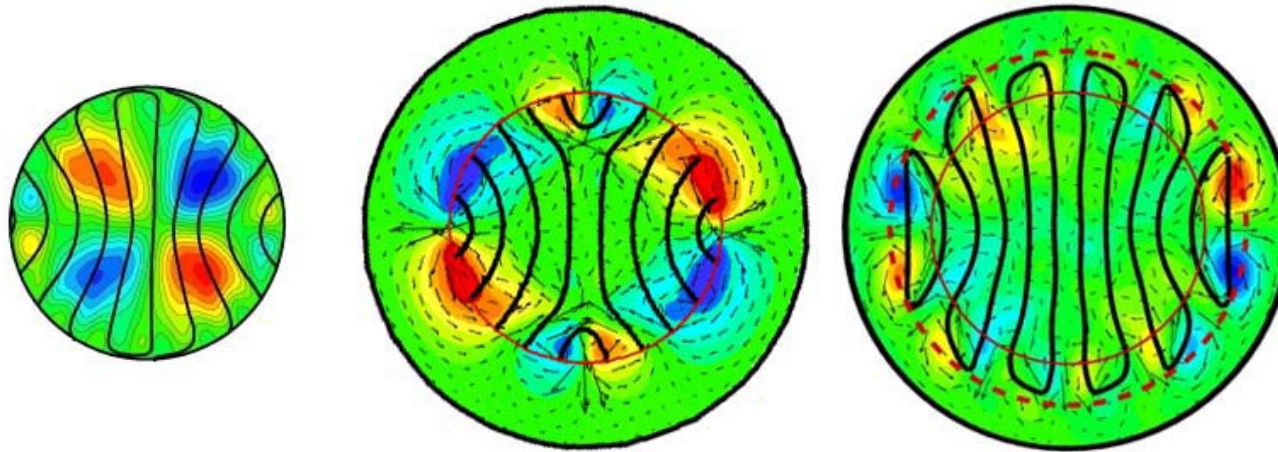
Sharp events similar in chaotic and periodic signals

Spectrogram





Role of mean flow

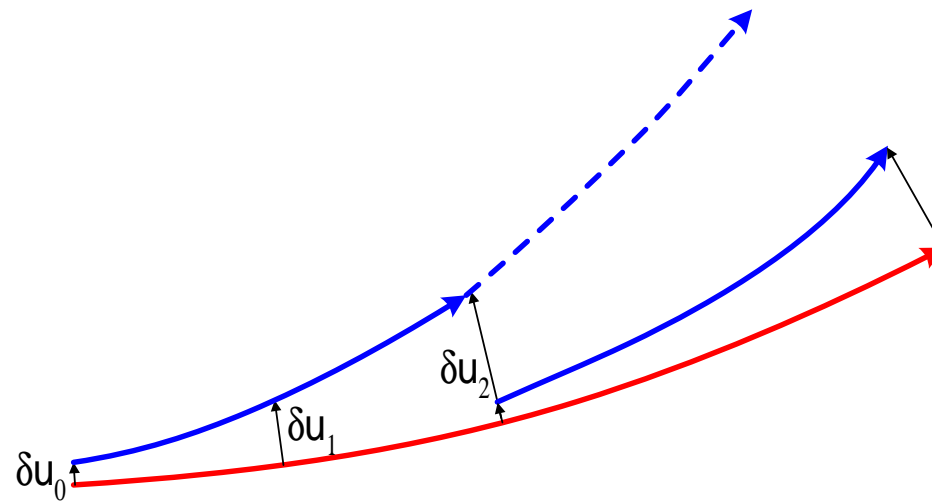


3 convection cells with different side wall conditions: (a) rigid; (b) finned; and (c) ramped. Case (a) is dynamic, the others static.

Sensitive dependence on initial conditions

- Lyapunov exponents:
 - ◇ Quantify the sensitivity to initial conditions
 - ◇ Define chaos
- Lyapunov vectors:
 - ◇ Associate sensitivity with specific events (defect creation, etc.)
 - ◇ Propagation of disturbances (Lorenz's question!)
- Lyapunov dimension:
 - ◇ Quantifies the number of active degrees of freedom
 - ◇ Scaling with system size may perhaps be used to define spatiotemporal chaos (microextensive chaos: Tajima and Greenside, 2002)

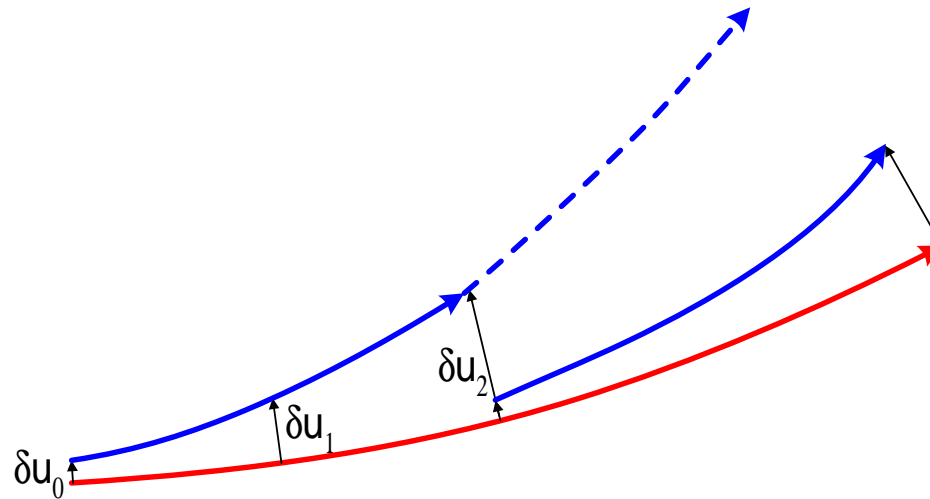
Lyapunov exponents



$$\delta u = \delta u_0 e^{\lambda_1 t}, \quad \lambda_1 = \lim_{t \rightarrow \infty} \frac{1}{t} \ln \frac{\delta u}{\delta u_0}$$

Line lengths $\rightarrow e^{\lambda_1 t}$, Areas $\rightarrow e^{(\lambda_1 + \lambda_2)t}$, Volumes $\rightarrow e^{(\lambda_1 + \lambda_2 + \lambda_3)t}, \dots$

Lyapunov exponents



$$\delta u = \delta u_0 e^{\lambda_1 t}, \quad \lambda_1 = \lim_{t \rightarrow \infty} \frac{1}{t} \ln \frac{\delta u}{\delta u_0}$$

Line lengths $\rightarrow e^{\lambda_1 t}$, Areas $\rightarrow e^{(\lambda_1 + \lambda_2)t}$, Volumes $\rightarrow e^{(\lambda_1 + \lambda_2 + \lambda_3)t}, \dots$

Lyapunov Dimension

$$D_L = \nu + \frac{1}{|\lambda_{\nu+1}|} \sum_{i=1}^{\nu} \lambda_i$$

where ν is the largest index such that the sum is positive.

Numerical Approach

Chaotic Boussinesq driving solution:

$$\begin{aligned} \frac{1}{\sigma} \left[\frac{\partial \vec{u}}{\partial t} + (\vec{u} \cdot \vec{\nabla}) \vec{u} \right] &= -\vec{\nabla} p + RT \hat{e}_z + \nabla^2 \vec{u} \\ \frac{\partial T}{\partial t} + (\vec{u} \cdot \vec{\nabla}) T &= \nabla^2 T \\ \vec{\nabla} \cdot \vec{u} &= 0 \end{aligned}$$

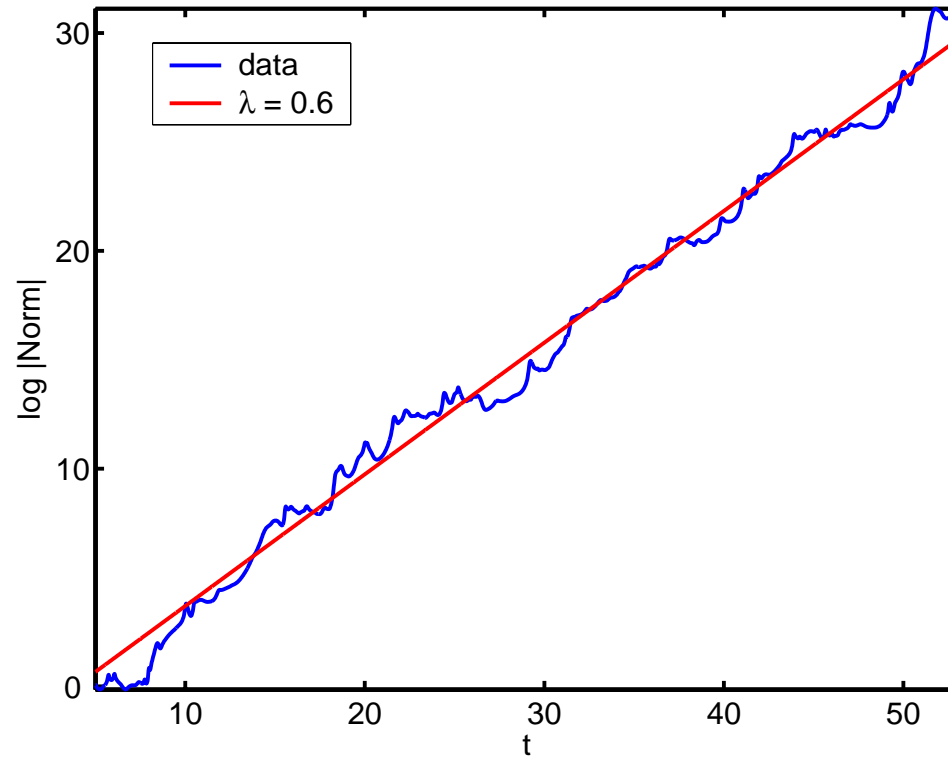
Linearized equations (tangent space equations):

$(\vec{u}, p, T) \rightarrow (\vec{u} + \delta \vec{u}_k, p + \delta p_k, T + \delta T_k)$, for $k = 1, \dots, n$

$$\begin{aligned} \frac{1}{\sigma} \left[\frac{\partial \delta \vec{u}_k}{\partial t} + (\vec{u} \cdot \vec{\nabla}) \delta \vec{u}_k + (\delta \vec{u}_k \cdot \vec{\nabla}) \vec{u} \right] &= -\vec{\nabla} \delta p_k + R \delta T \hat{e}_z + \nabla^2 \delta \vec{u}_k \\ \frac{\partial \delta T_k}{\partial t} + (\vec{u} \cdot \vec{\nabla}) \delta T_k + (\delta \vec{u}_k \cdot \vec{\nabla}) T &= \nabla^2 \delta T_k \\ \vec{\nabla} \cdot \delta \vec{u}_k &= 0 \end{aligned}$$

Simulations in an experimental geometry

$$\Gamma = 4.72, \sigma = 0.78, R = 6950$$



Experimentally realistic system is truly **chaotic**.

Lyapunov vector for spiral defect chaos

(from Keng-Hwee Chiam, Caltech thesis 2003)

Coarsening

Development of ordered state from random initial conditions

Much studied in statistical mechanics for relaxation to an ordered state in thermodynamic equilibrium.

Questions:

- Nature of asymptotic state
 - ◇ Ideal pattern or frozen disordered state?
- Coarsening dynamics
 - ◇ Often find power law growth of characteristic length scale $L \propto t^p$ with p often, but not always $\frac{1}{2}$
 - ◇ Phase diffusion or defect dynamics may be important

Coarsening to a stripe state

Coarsening in stripe systems is a hard problem

- Many types of defects: dislocations, disclinations, grain boundaries: hard to identify important dynamical processes
- A number of different arguments give slow growth $p \simeq \frac{1}{4}$, roughly consistent with numerical simulations,
- Recent experiments on very large relaxational systems suggest a dominant mechanism that is consistent with the observed scaling [Harrison et al. (2002)]

Coarsening to a state far from equilibrium has additional difficulties

- No energetic arguments to simplify discussion
- Asymptotic pattern not a priori known (wave number selection)

Progress so far

- Few experiments, none on rotationally invariant systems.
- Previous results are mainly based on numerical simulations of model equations.
- Much of the work is on relaxational models [Elder, Vinals, and Grant (1992)...]
- Two dimensional numerics on generalized Swift-Hohenberg models [MCC and Meiron (1995)] — both relaxational and nonrelaxational models.

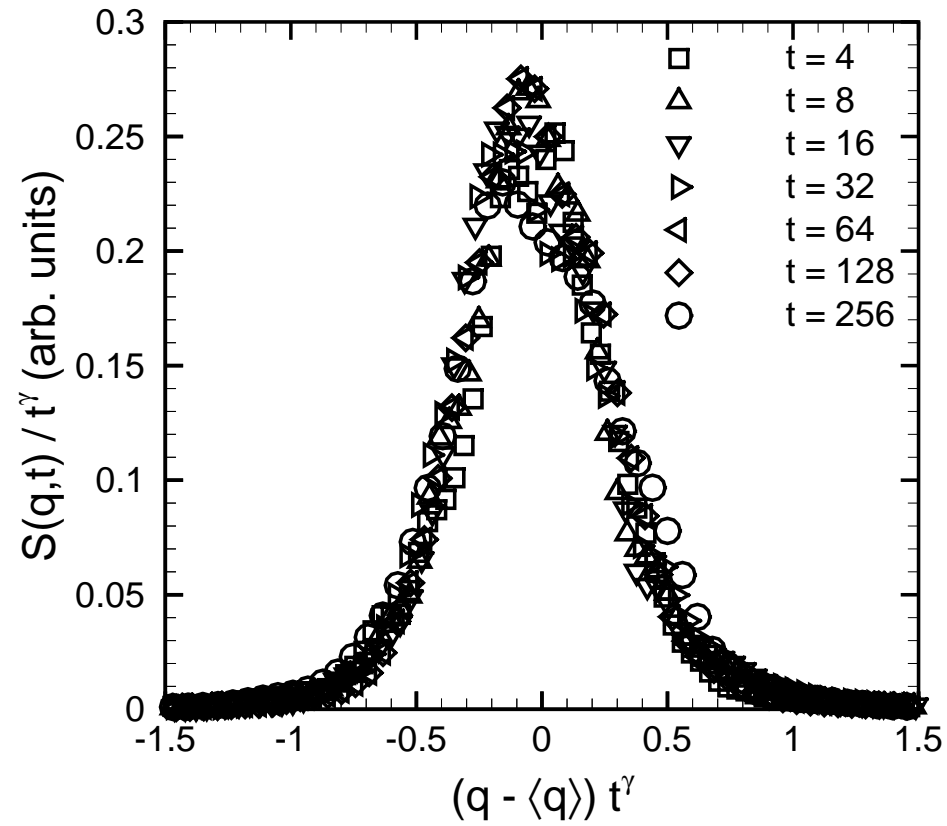
Rayleigh-Bénard simulations

Not very large! Limited to aspect ratios $\Gamma \sim 50$ to 100 — and therefore not very long times before finite size affects the dynamics.

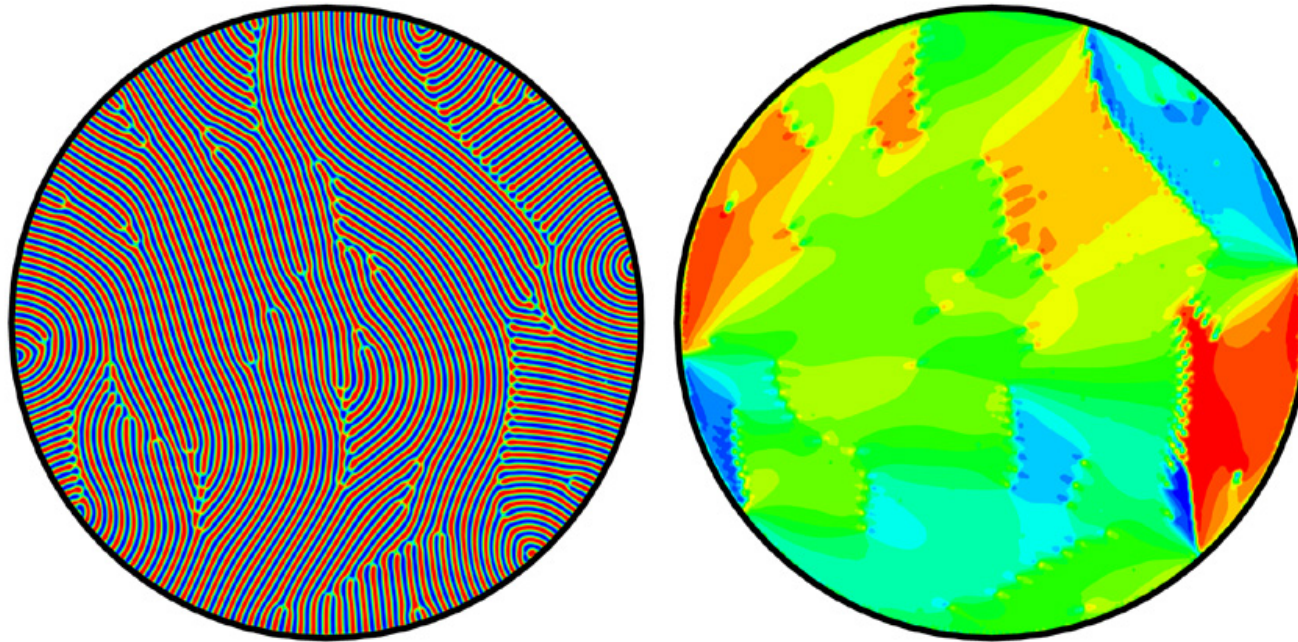
Main focus of work is on asymptotic state, and gross features of transient (e.g. whether $\gamma = \frac{1}{4}$ or $\frac{1}{2}$ not whether $\gamma = \frac{1}{4}$ or $\frac{1}{5}$)

$$R = 2169, \sigma = 1.4, \text{ and } \Gamma = 57$$

Structure factor



Orientation field correlation length

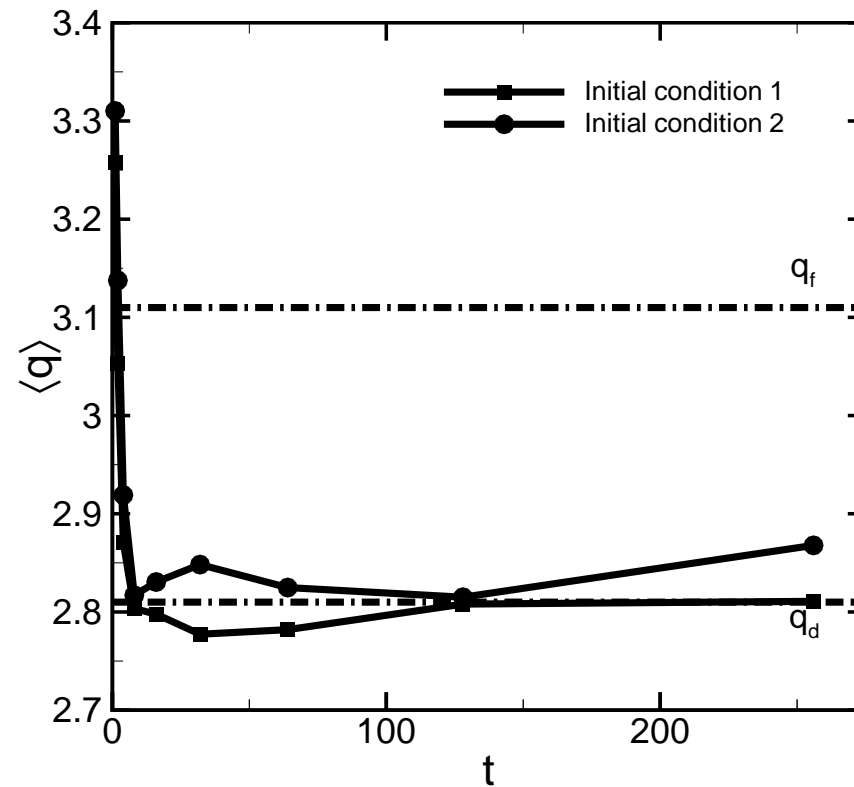


$$R = 2169, \sigma = 1.4, \Gamma = 57, t = 203$$

$$C_2 \left(|\vec{r} - \vec{r}'|, t \right) = \left\langle e^{i2(\theta(\vec{r},t) - \theta(\vec{r}',t))} \right\rangle$$

$$C_2 \sim e^{-r/\xi_0}$$

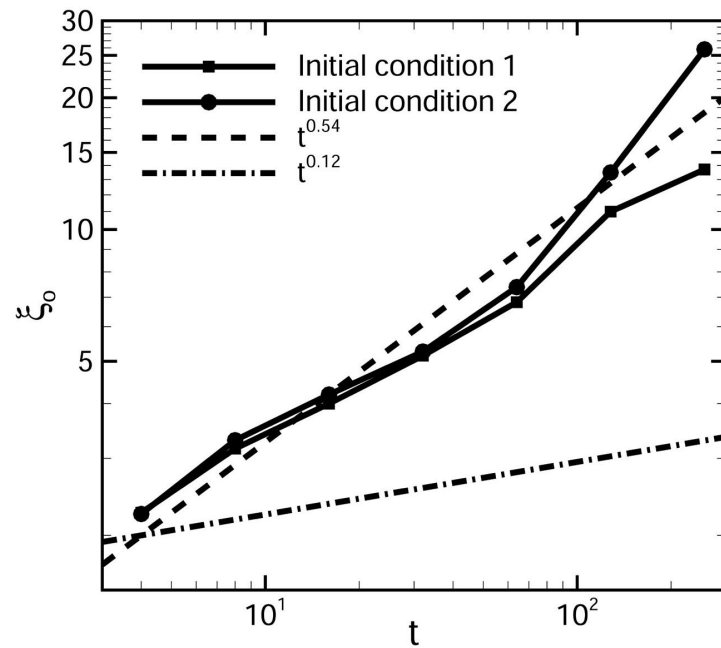
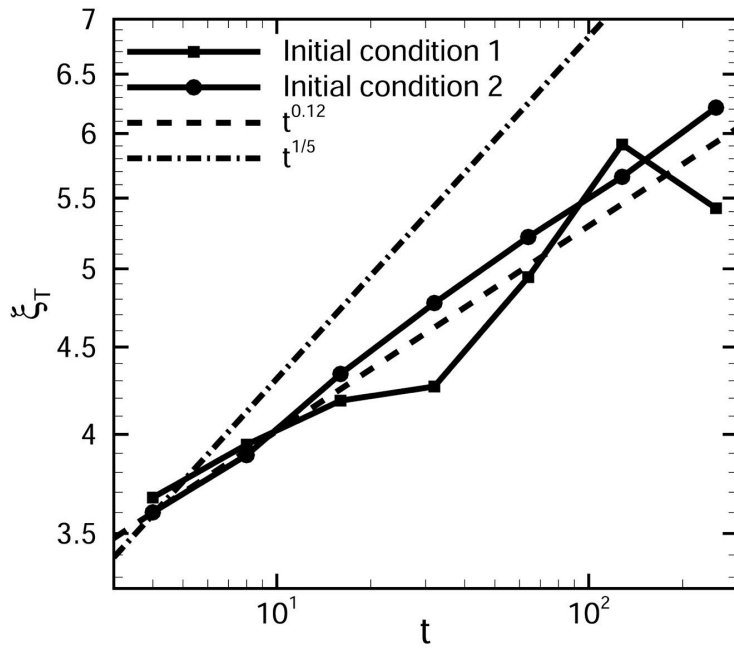
Mean wave number evolution



[q_d from Bodenschatz et al., Ann. Rev. Fluid Mech. 32 2000]

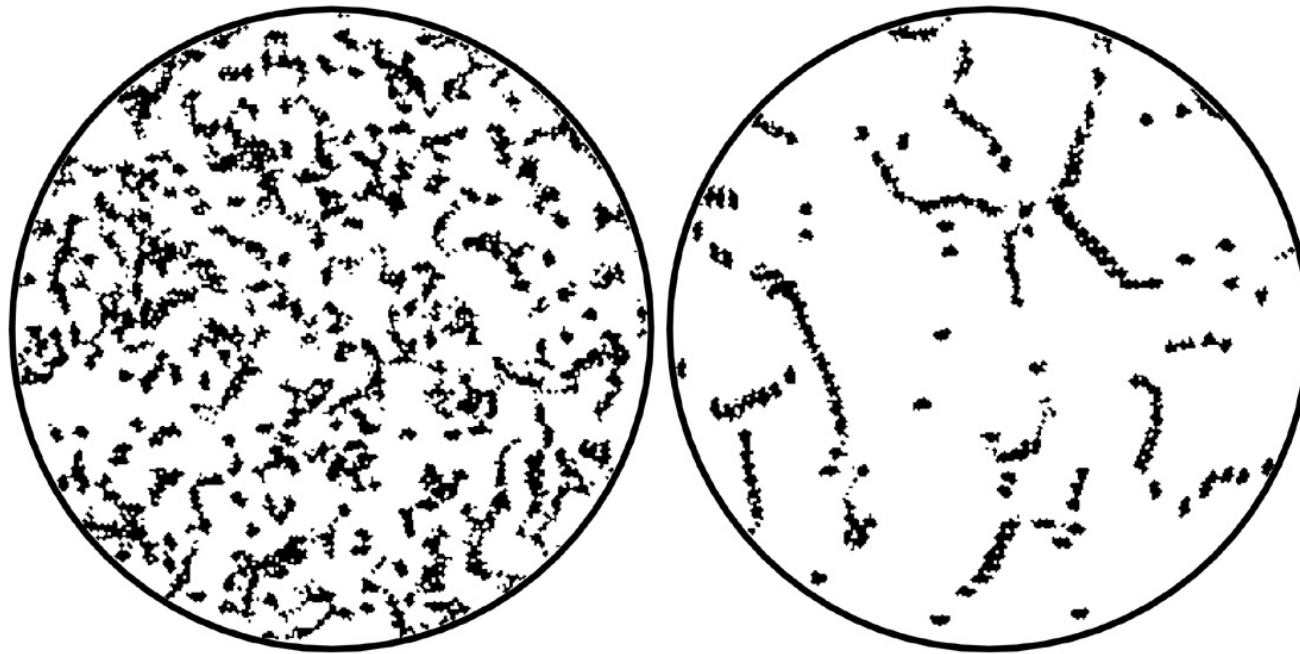
Wave number appears to approach dislocation selected value, not q_f .

Correlation lengths



Defect density

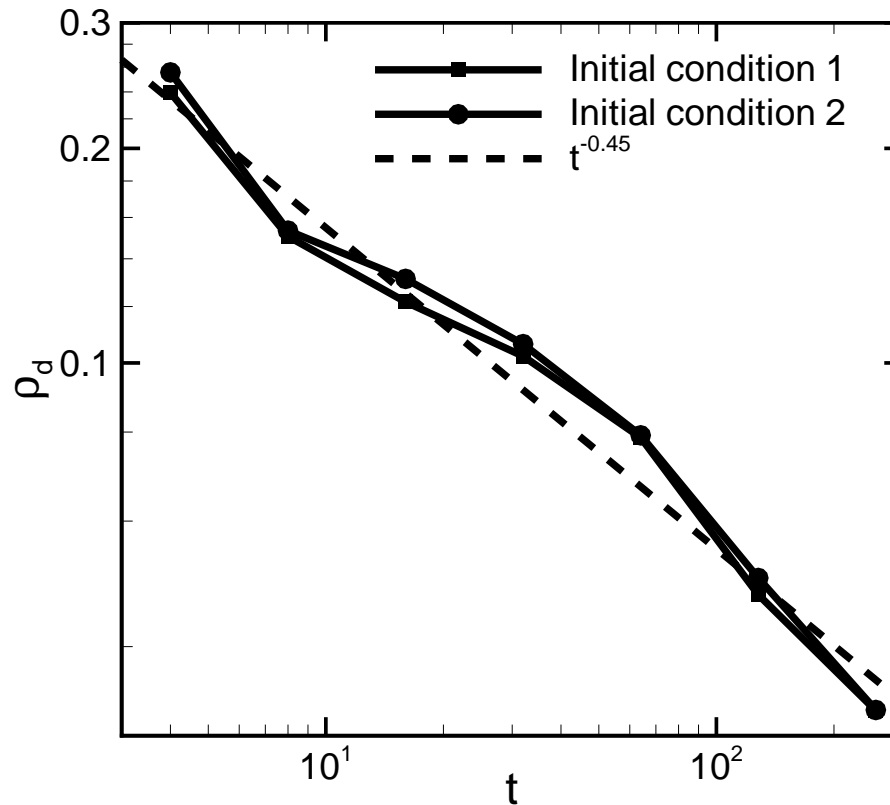
(defined as regions of large curvature)



$$R = 2169, \sigma = 1.4, \Gamma = 57, t = 8, 128$$

Defect lines (grain boundaries) clearly evident

Defect density



For isolated defects $L_D \sim \rho_D^{-1/2}$ so that $L_D \propto t^{1/4}$.

For defect lines ρ_d is the length of line, and the domain size scales as $t^{1/2}$

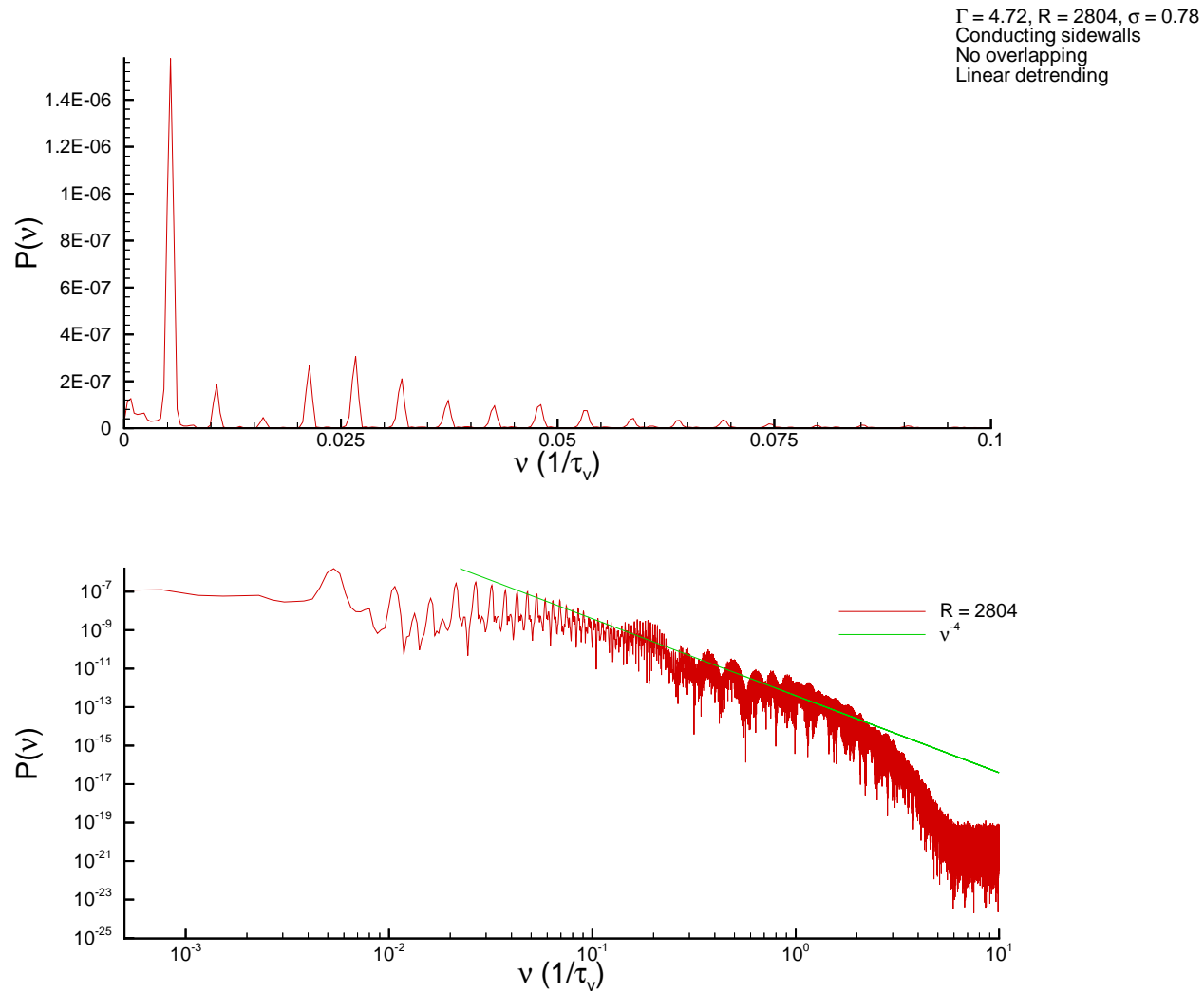
Conclusions

Numerical simulations on realistic experimental geometries complement experimental work and yield new insights

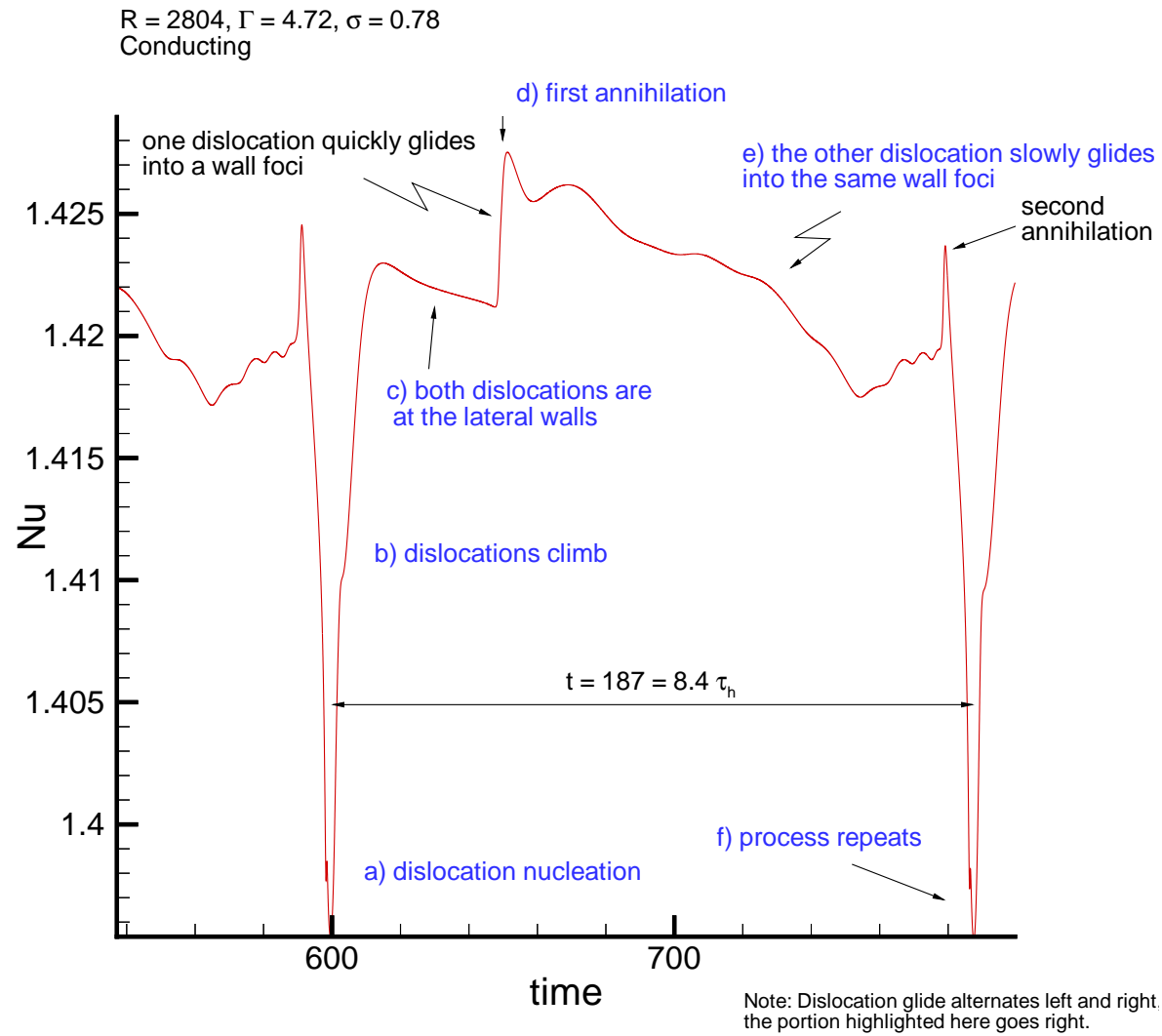
- Pattern chaos
 - ◇ Lower noise flows gives consistency of power spectrum with expectation based on deterministic chaos
 - ◇ Visualization of dynamics explains observed power law observed in spectrum
 - ◇ Confirmation of role of mean flow
- Lyapunov exponents and eigenvectors
 - ◇ Confirms early experiments were chaotic
 - ◇ Promising tools for studying spatiotemporal chaos
- Coarsening
 - ◇ Experiments needed!
 - ◇ Results largely consistent with previous nonrelaxational model simulations
 - ◇ Future work will investigate specific dynamics

THE END

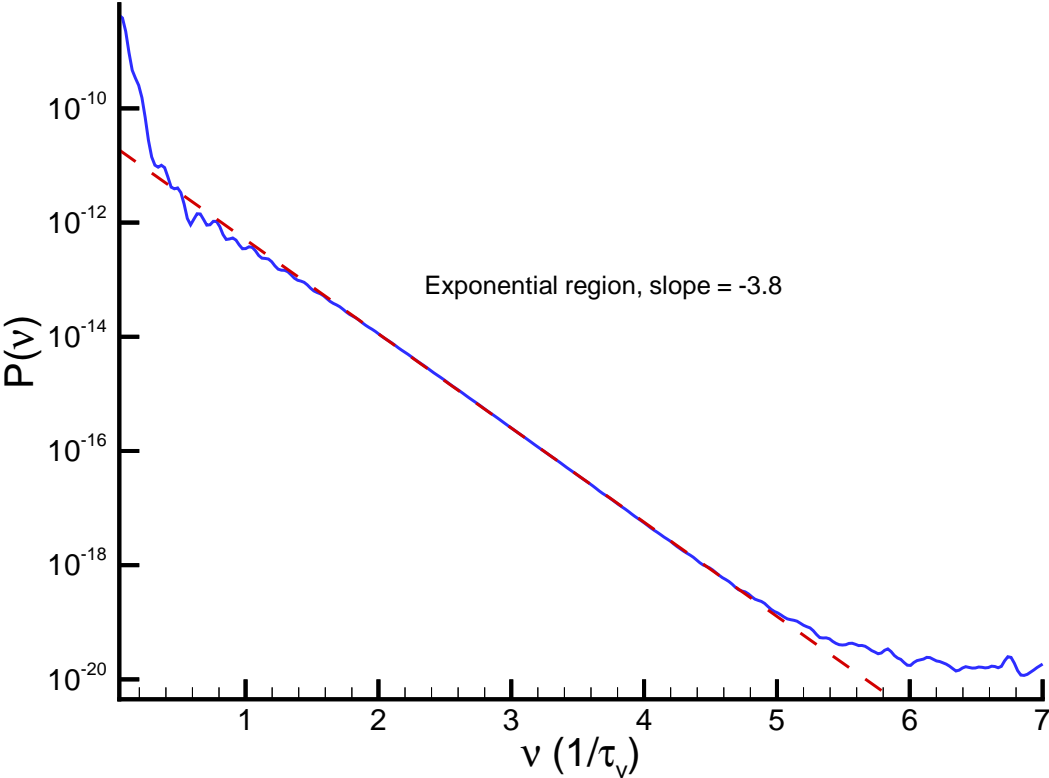
Power law spectra



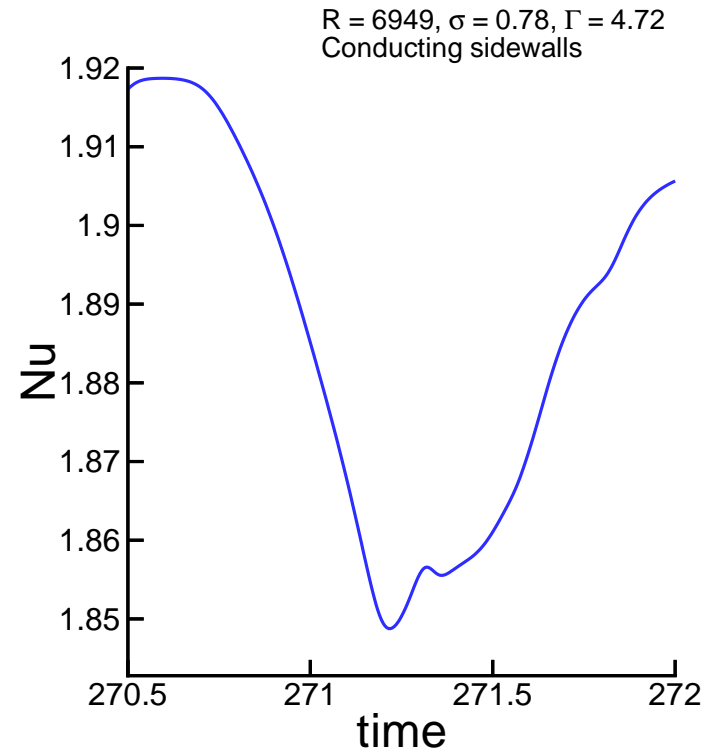
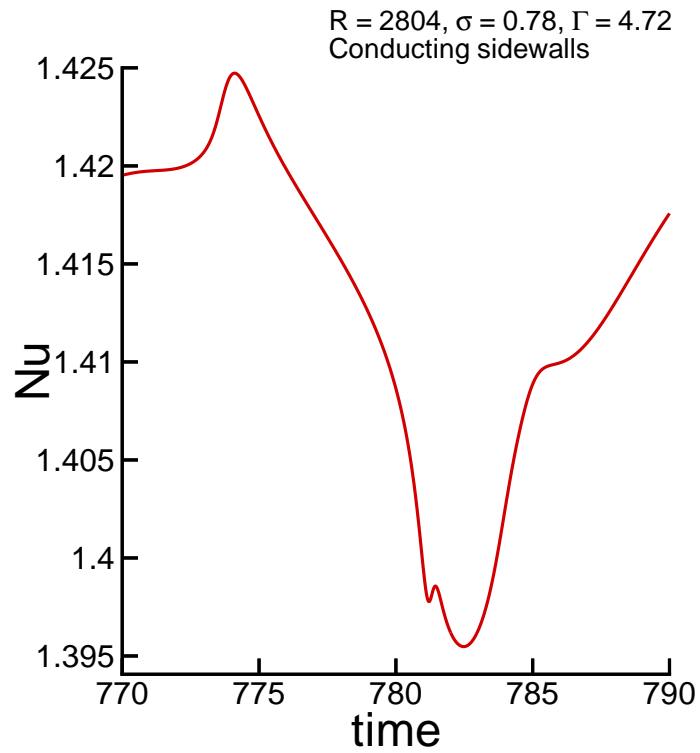
Time series $N(t)$



$R = 2804, \sigma = 0.78, \Gamma = 4.72$
Conducting sidewalls



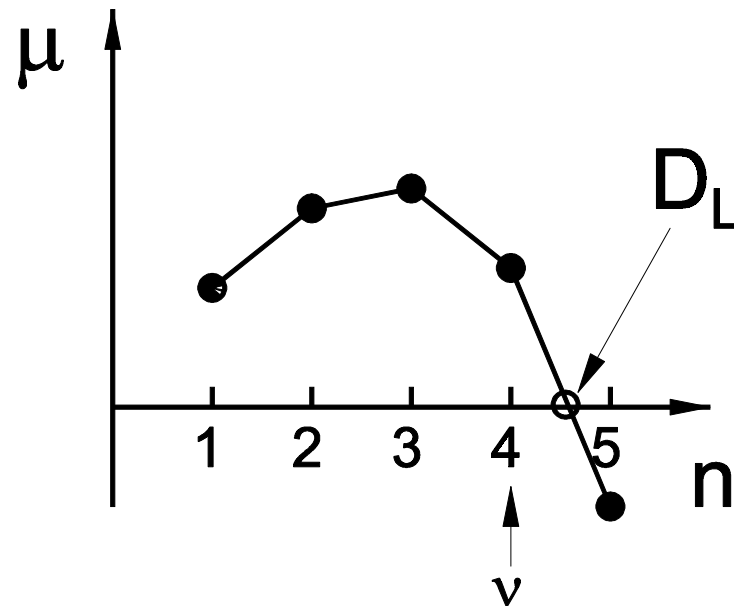
Compare periodic and chaotic events



Mechanism of Dynamics

- Pan-Am texture with roll pinch-off events creating dislocation pairs (Flow visualization, Pocheau, Le Gal, and Croquette 1985)
- Mean flow compresses rolls outside of stable band (Model equations, Greenside, MCC, Coughran 1985)
- Theoretical analysis of mean flow (Pocheau and Davidaud 1997)
- Numerical simulation of importance of mean flow (Paul, MCC, Fischer, and Greenside 2001)

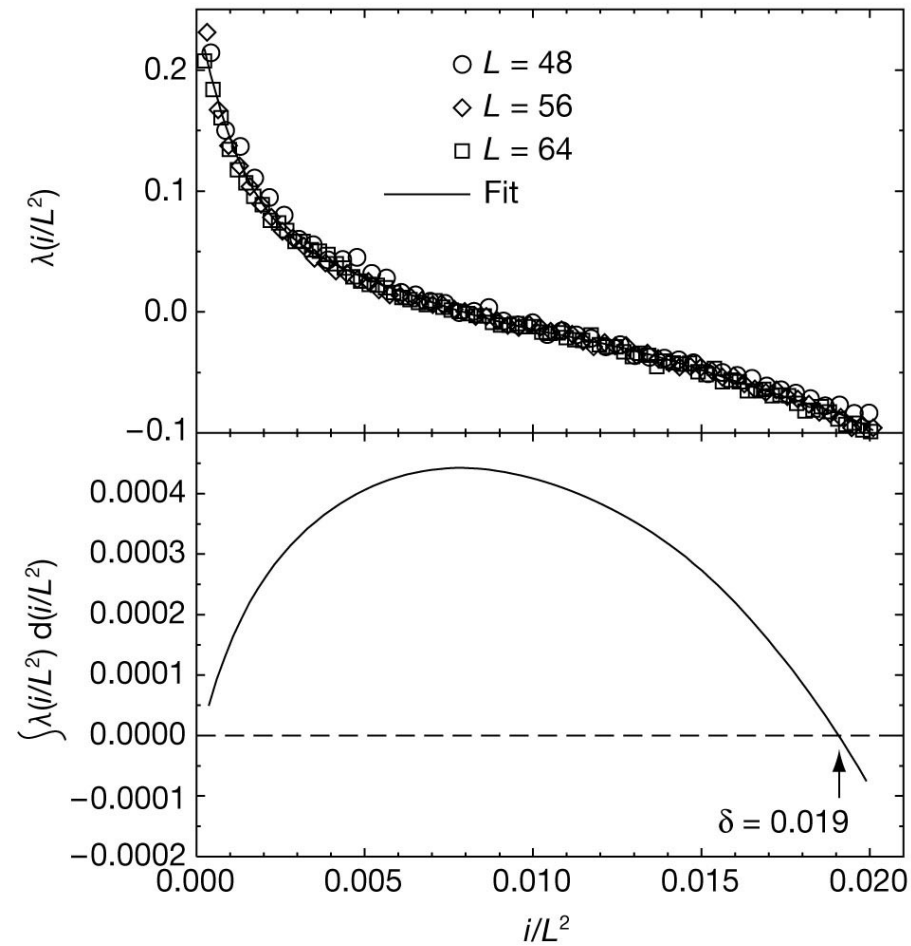
Lyapunov dimension



Define $\mu(n) = \sum_{i=1}^n \lambda_i$ ($\lambda_1 \geq \lambda_2 \dots$) with λ_i the i th Lyapunov exponent.

D_L is the interpolated value of n giving $\mu = 0$ (the dimension of the volume that neither grows nor shrinks under the evolution)

Lyapunov dimension for spiral defect chaos in a periodic geometry



(Egolf et al. 2000)

Previous Results

- Phase diffusion + focus wavenumber selection $D_{\perp} \rightarrow 0$ [MCC and Newell (1984)]

$$L \propto t^p, \quad p = \frac{1}{4}$$

- One dimensional numerics on Swift-Hohenberg model [Schober et al. (1986)]

$$p = \frac{1}{4}$$

Consistent with 1d phase diffusion with conserved phase winding [Rutenberg and Bray (1995)]

- Two dimensional numerics on Swift-Hohenberg model [Elder et al. (1992)...]

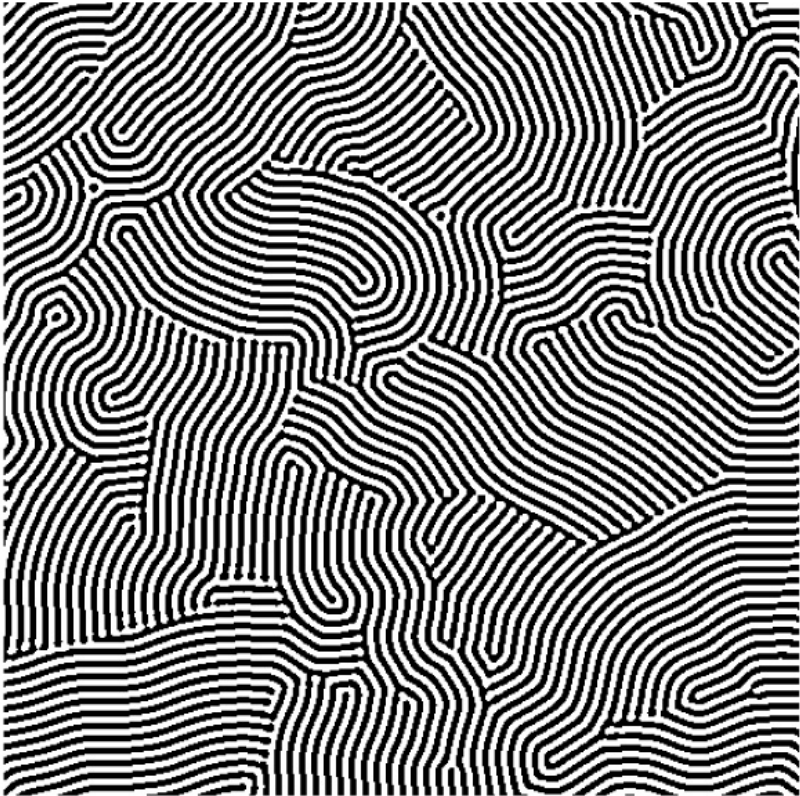
$$p \simeq \frac{1}{4} \quad \text{with noise;} \quad p \simeq \frac{1}{5} \quad \text{without noise}$$

Summary of results

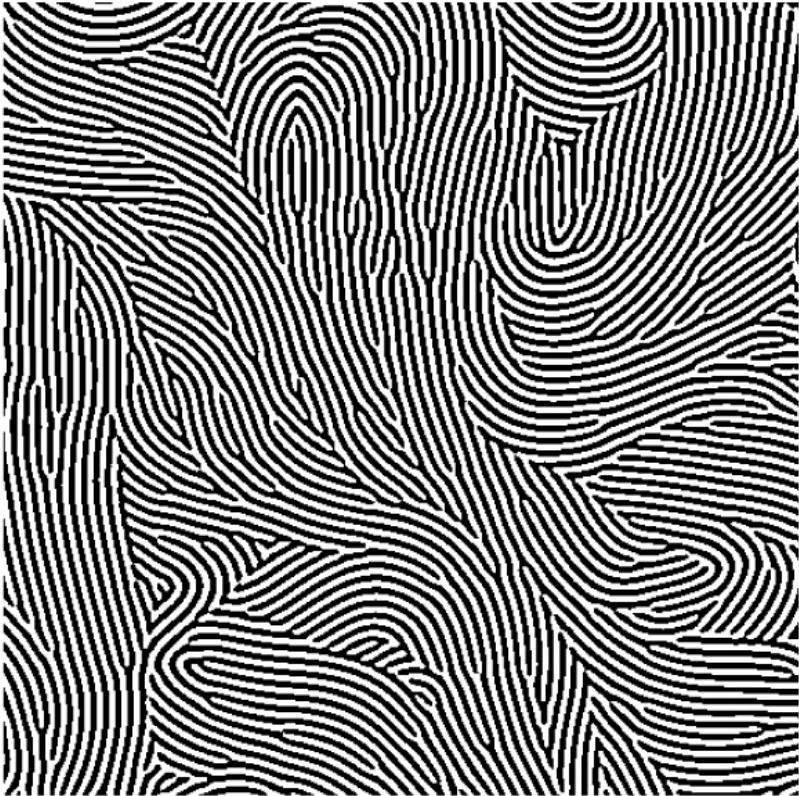
- For all cases without noise the growth of the correlation length measured from the width of the structure factor is consistent with $L \sim t^{1/5}$ ($\gamma \simeq 0.2$)
- For the non-relaxational models the correlation length measured from the orientational correlation function appears to follow a different scaling $L_o \sim t^{1/2}$
- The morphology and defect structure of the patterns appeared to be different in the relaxational and non-relaxational cases
 - ◇ Relaxational: predominance of patches of straight stripes with sharp boundaries showing up as defect lines
 - ◇ Non-relaxational: predominance of smoothly curved stripes with many isolated dislocation defects
- For the non-relaxational models the asymptotic wave number is **not** consistent with $D_{\perp}(q) = 0$ but appears to be the wave number q_d for which dislocation climb does not occur.

Morphology

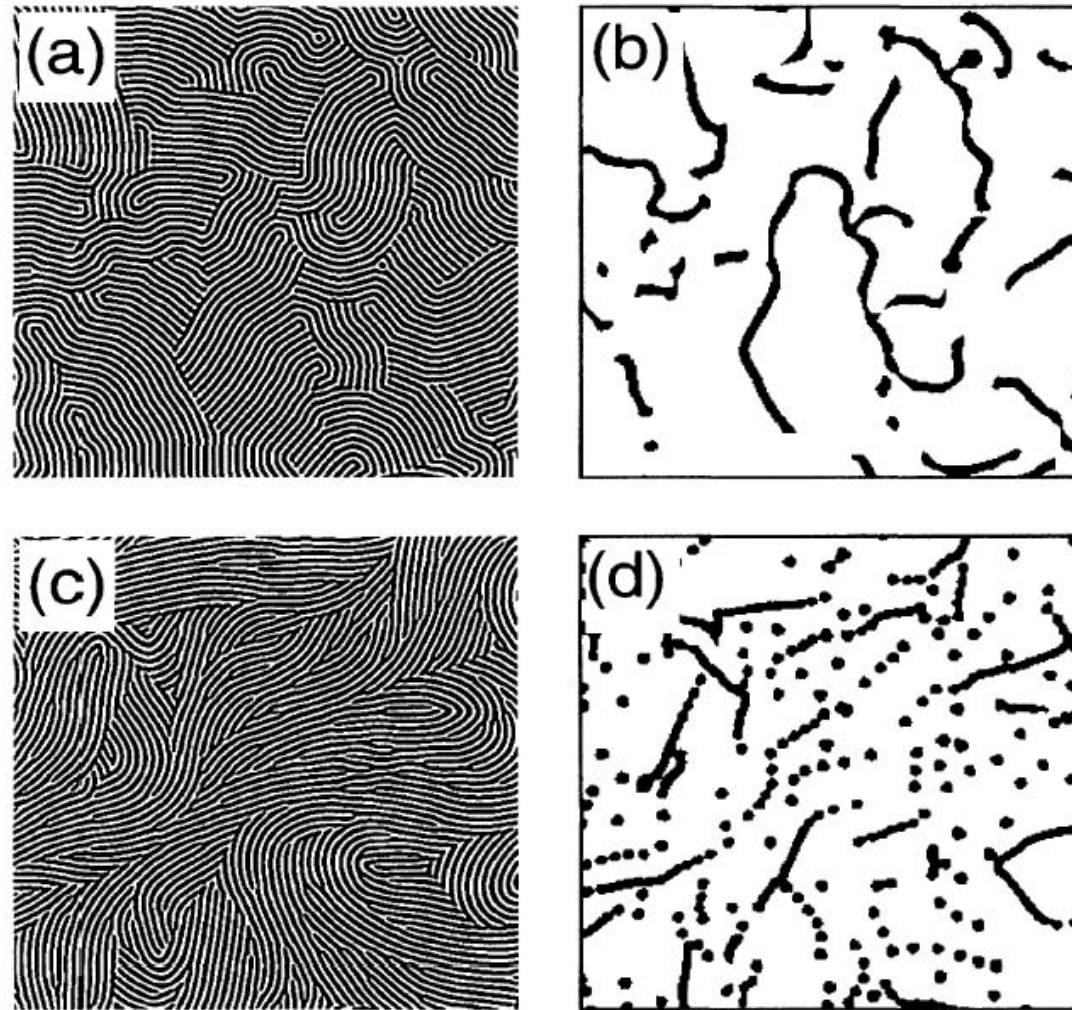
Relaxational



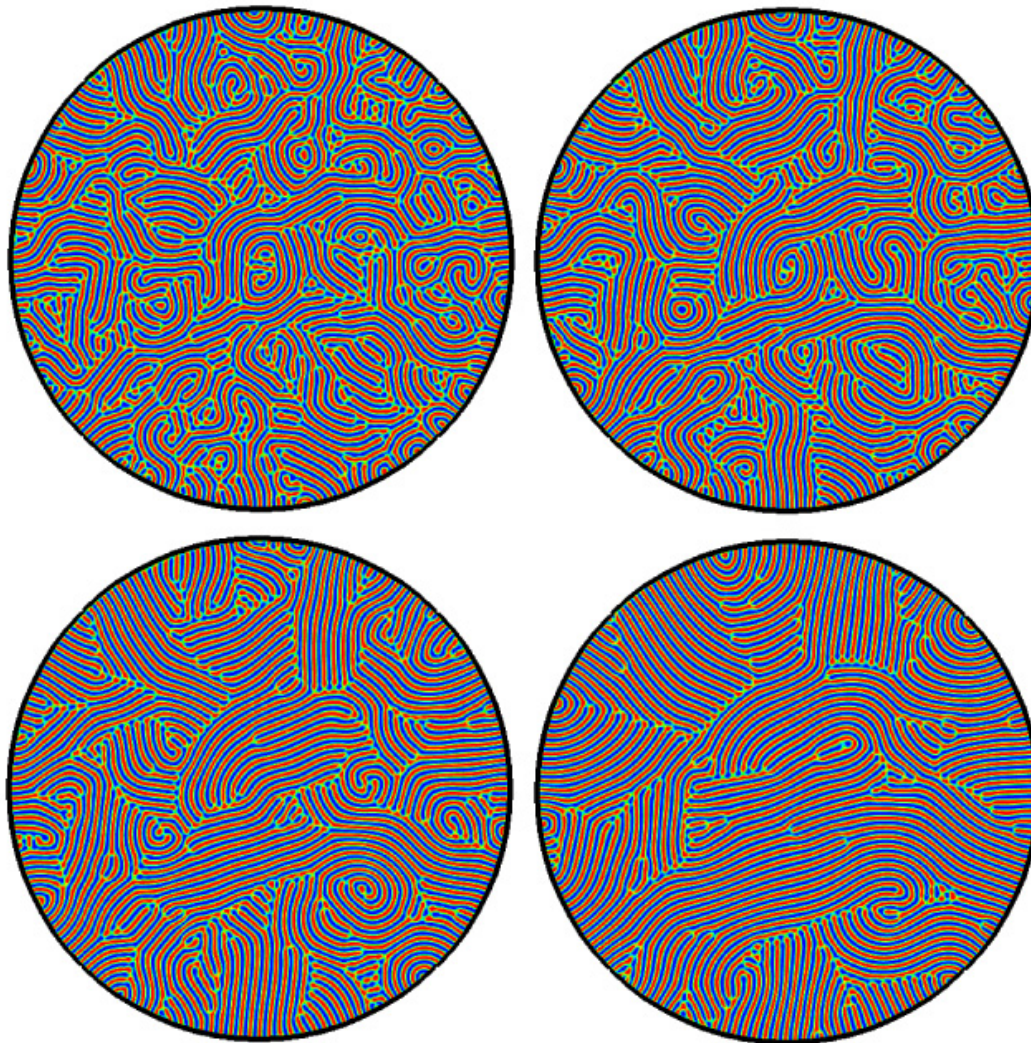
Non-relaxational



Defects



(a),(b) relaxational; (c),(d) non-relaxational



$R = 2169, \sigma = 1.4, \Gamma = 57, t = 16, 32, 64, \text{ and } 128$

Conclusions

Numerical simulations on realistic experimental geometries complement experimental work and yield new insights

- Pattern chaos
 - ◇ Lower noise flows gives consistency of power spectrum with expectation based on deterministic chaos
 - ◇ Visualization of dynamics explains observed power law observed in spectrum
 - ◇ Confirmation of role of mean flow
- Lyapunov exponents and eigenvectors
 - ◇ Confirms early experiments were chaotic
 - ◇ Promising tools for studying spatiotemporal chaos
- Coarsening
 - ◇ Experiments needed!
 - ◇ Results largely consistent with previous nonrelaxational model simulations
 - ◇ Future work will investigate specific dynamics